Japanese Journal of Physiology, **50**, 371–380, 2000

Closed-Loop Identification of Carotid Sinus Baroreflex Transfer Characteristics Using Electrical Stimulation

Toru KAWADA, Takayuki SATO, Masashi INAGAKI, Toshiaki SHISHIDO, Teiji TATEWAKI, Yusuke YANAGIYA, Can ZHENG, Masaru SUGIMACHI, and Kenji SUNAGAWA

Department of Cardiovascular Dynamics, National Cardiovascular Center Research Institute, Suita, 565–8565 Japan

Abstract: Although random aortic pressure (AOP) perturbation according to a binary white noise sequence enables us to estimate open-loop dynamic characteristics of the carotid sinus baroreflex under closed-loop conditions, the necessity of arterial catheter implantation limits the applicability of this method in freely moving animal experiments. Thus, we explored a closed-loop system identification method using electrical stimulation. In 6 anesthetized and vagotomized rabbits, we stimulated the aortic depressor nerve with a binary white noise sequence (0–10 Hz) under baroreflex closed-loop conditions while measuring cardiac sympathetic nerve activity (SNA) and AOP. We used a closed-loop identification method to estimate the peripheral arc transfer function from SNA to AOP. The peripheral arc transfer function approximated a second-order low-pass filter and its fitted parameters did not differ from those obtained by an open-loop identification method (dynamic gain: 1.16±0.32 vs. 1.02±0.11; natural frequency: 0.08±0.03 vs. 0.09±0.03 Hz; damping ratio: 1.53±0.15 vs. 1.57±0.21). In 6 different rabbits, we applied intermittent rapid pacing (396 beats/min) under baroreflex closed-loop conditions to estimate the neural arc transfer function from AOP to SNA. The neural arc transfer function approximated a first-order high-pass filter and its fitted parameters did not differ from those obtained by an open-loop identification method (dynamic gain: −1.15±0.45 vs. −1.06±0.05; corner frequency: 0.12±0.05 vs. 0.13±0.03 Hz). In conclusion, the closed-loop identification method using electrical stimulation is effective to estimate the neural and peripheral arc transfer functions. [Japanese Journal of Physiology, 50, 371–380, 2000]

Key words: systems analysis, transfer function, sympathetic nerve activity, aortic depressor nerve, rapid pacing.

Dynamic characteristics of the sympathetic arterial baroreflex may be divided into neural arc and peripheral arc components [1]. The neural arc represents an input-output relationship between baroreceptor pressure input and efferent sympathetic nerve activity (SNA), whereas the peripheral arc represents an input-output relationship between SNA and aortic pressure (AOP). Knowledge of the dynamic characteristics of these two arcs is important for understanding the stability and quickness of arterial pressure control [1]. However, in order to estimate the open-loop transfer functions of these two arcs, it was necessary to isolate baroreceptor regions and open the baroreflex feedback loop [1, 2]. To avoid isolating baroreceptor regions, closed-loop system identification methods using an impulse pressure input and a stepwise pressure input have been developed [3, 4]. We also established a closed-loop system identification method using exogenous arterial pressure perturbation according to a binary white noise sequence in estimating baroreflex open-loop transfer functions [5]. However, these methods necessitate exogenous pressure perturbation through a catheter, which limits the applicability of these methods in experiments involving freely moving

Received on April 6, 2000; accepted on May 18, 2000
Correspondence should be addressed to: Toru Kawada, Department of Cardiovascular Dynamics, National Cardiovascular Center Research Institute, 5–7–1 Fujishirodai, Suita, 565–8565, Japan.

conscious animals. Infection and embolization associated with arterial catheter implantation represent other limiting factors for the use of these methods in long-term chronic animal experiments. To overcome these problems, we examined the usefulness of electrical stimulation in identifying baroreflex open-loop transfer functions under closed-loop conditions. Given that electrical stimulation can be performed wirelessly using an implantable electrical stimulator with a small battery, it has potential advantages over catheter implantation when used in freely moving conscious animal experiments. We used aortic depressor nerve (ADN) stimulation [6] and rapid cardiac pacing [7] to perturb the arterial baroreflex system under closed-loop conditions. The aim of the present study was to verify the closed-loop system identification method using electrical stimulation by comparing the estimated baroreflex open-loop transfer functions with those obtained from a conventional open-loop system identification method.

MATERIALS AND METHODS

Surgical preparations. Animals were cared for in accordance with the Guiding Principles for the Care and Use of Animals in the Field of Physiological Sciences, approved by the Physiological Society of Japan. Twelve Japanese white rabbits weighing between 2.2 and 3.2 kg were anesthetized via intravenous injection (2 ml/kg) of a mixture of urethane (250 mg/ml) and α-chloralose (40 mg/ml), and mechanically ventilated with oxygen-enriched room air. Supplemental anesthetics were injected as necessary (0.5 ml/kg) to maintain an appropriate depth of anesthesia. AOP was recorded using a high-fidelity pressure transducer (Millar Instruments, Houston, TX) inserted from the right femoral artery. Bilateral vagi and aortic depressor nerves were sectioned at the neck to eliminate baroreflexes from cardiopulmonary regions and the aortic arch. We isolated the bilateral carotid sinuses from systemic circulation by ligating the internal, external, and common carotid arteries, as well as other small branches originating from the carotid sinus regions. The isolated carotid sinuses were filled with warmed saline and connected to a servo-controlled piston pump (model ET-126A, Labworks, Costa Mesa, CA) via catheters inserted from the common carotid arteries. Intra-carotid sinus pressure (CSP) was measured from a sidearm of the catheter inserted into the carotid sinuses. We sectioned the left cardiac sympathetic nerve via a midline thoracotomy and attached a pair of platinum electrodes to the central end of the sectioned nerve to record SNA. To prevent desiccation and provide insulation, the electrodes and nerve were immersed in a mixture of white petrolatum (Vaseline) and liquid paraffin. Pancuronium bromide (0.5 mg/kg) was administered to prevent contamination of muscular activity in the nerve recording signal. The preamplified nerve signal was full-wave rectified and then low-pass filtered with a cut-off frequency of 30 Hz to quantify nerve activity. Body temperature was maintained at 37°C with a heating pad throughout the experiment.

In the ADN stimulation group ($n=6$), we attached a pair of platinum electrodes to the central end of the sectioned right ADN for stimulation. The right ADN was identified by a depressor response in AOP during brief electrical stimulation of the nerve. The electrodes and nerve were immersed in a mixture of white petrolatum (Vaseline) and liquid paraffin. We wrapped grounded aluminum foil around the neck of the animal to eliminate contamination of the stimulation signal in the SNA recording. In the rapid pacing group ($n=6$), we attached a pair of fine stainless wire electrodes to the right atrial appendage via a pericardial incision for electrical pacing. We put grounded aluminum foil on the pericardium to eliminate contamination of the pacing signal in the SNA recording.

Protocols. We performed open-loop and closed-loop identification protocols in both the ADN stimulation and rapid pacing groups. When baroreflex closed-loop conditions were required, CSP was servo-controlled to precisely follow AOP. The time constant of the servo control system was 50 ms, which was sufficiently short to impose pressure perturbation up to the highest frequency of physiological interest (0.7 Hz) in the present study.

In the open-loop identification protocol of the ADN stimulation group, we perturbed CSP according to a binary white noise signal [5, 8–12]. The switching interval of the binary sequence was set at 700 ms so that the input power spectrum was relatively flat up to 0.7 Hz. The mean CSP (103.2±9.7 mmHg) was determined by an equilibrium pressure between CSP and AOP obtained under baroreflex closed-loop conditions. The peak-to-peak amplitude of CSP perturbation was 49.6±7.6 mmHg.

In the closed-loop identification protocol of the ADN stimulation group, we stimulated the right ADN according to a binary white noise signal [6] with a switching interval of 700 ms. The 10-Hz ADN stimulation was switched either on or off according to the binary sequence. The pulse duration of nerve stimulation was set at 2 ms. The amplitude of nerve stimulation ranged from 1.5 to 3 V. With this setting, 10-Hz tonic ADN stimulation decreased AOP by about

30 mmHg when the carotid sinus baroreflex was disabled by fixing CSP at a constant pressure.

In the open-loop identification protocol of the rapid pacing group, we perturbed CSP according to a binary white noise signal [5, 8–12] with a switching interval of 700 ms. The mean CSP (89.2±17.1 mmHg) and peak-to-peak amplitude of CSP perturbation (45.1±10.8) were adjusted to the range of AOP response during a preliminary application of the intermittent rapid pacing.

In the closed-loop identification protocol of the rapid pacing group, we paced the heart according to a binary white noise signal [7] with a switching interval of 700 ms. The rapid atrial pacing (396 beats/min) was switched either on or off according to the binary sequence. When the rapid pacing was turned off, the heart beat according to its own rhythm. The pulse duration and amplitude of atrial pacing were set at 500 μs and 2 V, respectively.

To reduce the likelihood of bias or systematic error in our identification approach, we randomized the order of the open-loop and closed-loop identification protocols among the animals. We used different sequences of binary white noise for different protocols and different animals. In each protocol, we recorded CSP, SNA, AOP and the command signal for ADN stimulation or atrial pacing for 10 min. The recordings were digitized at a sampling rate of 200 Hz using a 12-bit analog-to-digital converter and stored on the hard disk of a dedicated laboratory computer system (NEC PC-9801FA, Tokyo, Japan).

Data analysis.

Open-loop system identification method. The data were analyzed beginning at 2 min after the onset of CSP perturbation. The neural arc and peripheral arc transfer functions were estimated by means of an analysis for one-input, one-output systems. We resampled the input-output data pairs at 10 Hz and segmented them into eight sets of 50% overlapping bins of 1,024 data points each [13]. For each segment, the linear trend was removed and the Hanning window was applied. We performed a fast Fourier transform to obtain the frequency spectra of input and output signals [14]. We then ensemble averaged the input power [$S_{X\cdot X}(f)$], output power [$S_{Y\cdot Y}(f)$], and crosspower between the input and output signals [$S_{Y\cdot X}(f)$] over the eight segments. Finally, we obtained a transfer function [$H(f)$] using the following equation [8].

$$H(f)=\frac{\mathrm{E}[S_{Y\cdot X}(f)]}{\mathrm{E}[S_{X\cdot X}(f)]} \tag{1}$$

where E[·] represents the ensemble average operation. We also calculated the magnitude-squared coherence function. The coherence function [$Coh(f)$] is a measure of linear dependence between the input and output signals in the frequency domain. It was calculated using the following equation [8].

$$Coh\,(f)=\frac{\left|\mathrm{E}[S_{Y\cdot X}(f)]\right|^2}{\mathrm{E}[S_{X\cdot X}(f)]\mathrm{E}[S_{Y\cdot Y}(f)]}. \tag{2}$$

Closed-loop system identification method. Figure 1A shows a schema of the closed-loop identification method during ADN stimulation. $H_N(f)$ and $H_P(f)$ denote the neural arc and peripheral arc transfer functions of the carotid sinus baroreflex, respectively. SNA(f) and AOP(f) are the Fourier transforms of SNA and AOP, respectively. $U(f)$ represents the SNA component that is not mediated by the neural arc. $V(f)$ represents the AOP fluctuation that is not mediated by the peripheral arc. When we stimulate the ADN, SNA decreases through the aortic baroreflex. $D(f)$ and $H_D(f)$ represent a command sequence of the ADN stimulation and the transfer function from ADN stimulation to the SNA response, respectively. Although $H_D(f)$ can also be interpreted as a neural arc transfer function, its input is an electrical stimulation rather than a pressure perturbation. Thus, we did not characterize $H_D(f)$ in the present study. Under these conditions, the carotid sinus baroreflex can be expressed in the frequency domain as:

$$\mathrm{SNA}(f)=H_N(f)\mathrm{AOP}(f)+U(f)+H_D(f)D(f), \tag{3}$$

$$\mathrm{AOP}(f)=H_P(f)\mathrm{SNA}(f)+V(f). \tag{4}$$

Calculating the ensemble average of the crosspower between the terms of Eq. 4 and $D(f)$, we obtain:

$$\mathrm{E}[S_{\mathrm{AOP}\cdot D}(f)]=H_P(f)\mathrm{E}[S_{\mathrm{SNA}\cdot D}(f)]+\mathrm{E}[S_{V\cdot D}(f)]. \tag{5}$$

When $D(f)$ is a white noise sequence, $\mathrm{E}[S_{V\cdot D}(f)]$ asymptotically diminishes by virtue of the statistical independence between signals $D(f)$ and $V(f)$. Therefore, we can obtain an unbiased estimate of $H_P(f)$ as follows [15].

$$H_P(f)=\frac{\mathrm{E}[S_{\mathrm{AOP}\cdot D}(f)]}{\mathrm{E}[S_{\mathrm{SNA}\cdot D}(f)]}. \tag{6}$$

Figure 1B shows a schema of the closed-loop identification during rapid pacing. The notations are the same as those in Fig. 1A except for the rapid pacing command sequence, $R(f)$, and the transfer function from rapid pacing to AOP response, $H_R(f)$. The dashed line between $R(f)$ and $H_P(f)$ indicates that the rapid pacing deprives the peripheral arc transfer function of the heart rate control component. Under these conditions, $H_P(f)$ is no longer time invariant. Nevertheless, when we focus on the neural arc transfer func-

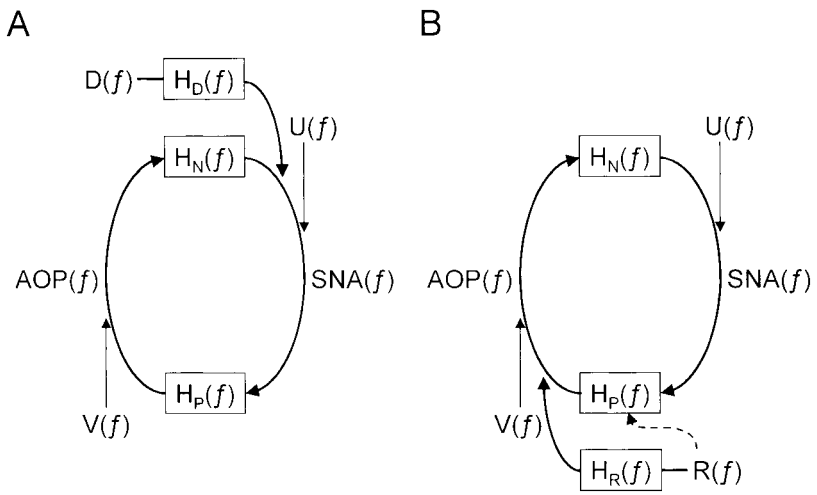

Fig. 1. Schemata of closed-loop system identification method in the frequency domain. $H_N(f)$ and $H_P(f)$ indicate neural arc and peripheral arc transfer functions of the carotid sinus baroreflex, respectively. AOP(f) and SNA(f) are Fourier transforms of aortic pressure (AOP) and sympathetic nerve activity (SNA), respectively. $U(f)$ and $V(f)$ represent unknown internal noise components in SNA(f) and AOP(f), respectively. **A**: Closed-loop identification using aortic depressor nerve (ADN) stimulation. $D(f)$ and $H_D(f)$ indicate Fourier transform of the command sequence of ADN stimulation and the transfer function from ADN stimulation to the SNA response, respectively. **B**: Closed-loop identification using rapid pacing. $R(f)$ and $H_R(f)$ indicate Fourier transform of the command sequence of intermittent rapid pacing and the transfer function from rapid pacing to AOP response, respectively. Since intermittent rapid pacing parametrically affects $H_P(f)$ (dashed line), $H_P(f)$ becomes time variant under these conditions.

tion, SNA(f) can be expressed as:

$$\mathrm{SNA}(f)=H_N(f)\mathrm{AOP}(f)+U(f)\,. \tag{7}$$

By using the statistical independence between $R(f)$ and $U(f)$, we can estimate $H_N(f)$ as follows [15].

$$H_N(f)=\frac{\mathrm{E}[S_{\mathrm{SNA\cdot R}}(f)]}{\mathrm{E}[S_{\mathrm{AOP\cdot R}}(f)]}. \tag{8}$$

Statistical analysis. All data are presented as means±SD values. As the magnitude of SNA varied among animals depending on the recording condition, it was described in arbitrary units. The transfer functions were normalized in each animal using the same normalization coefficient so that the differences in transfer gain between the open-loop and closed-loop protocols, if any, persist after the normalization. According to previous studies [1, 5, 16, 17], we parameterized $H_N(f)$ by fitting a first-order high-pass filter in the frequency range from 0.01 to 0.7 Hz by means of iterative nonlinear least-squares fitting (see APPENDIX). We parameterized $H_P(f)$ by fitting a second-order low-pass filter in the frequency range from 0.01 to 0.7 Hz (see APPENDIX). We used a paired t-test [18] to compare the fitted parameters between the open-loop and closed-loop identification protocols. The associated p values are shown along with the estimated parameters.

RESULTS

ADN stimulation group

Figure 2 presents typical recordings obtained from the ADN stimulation group, showing CSP, command signal for ADN stimulation, SNA and AOP. The left and right panels correspond to the open-loop and closed-loop identification protocols, respectively. In the open-loop identification protocol, we perturbed CSP according to a binary white noise sequence, while not stimulating the ADN. When CSP was raised, SNA decreased and AOP subsequently decreased. When CSP was decreased, the opposite responses were observed. In the closed-loop identification protocol, CSP was servo-controlled to precisely follow changes in AOP, thereby establishing baroreflex closed-loop conditions. We stimulated ADN according to a binary white noise sequence. SNA and AOP changed in response to the ADN stimulation. Although SNA might also respond to changes in CSP, the relationships among these signals could not be differentiated by a simple inspection of the time series data.

Figure 3 shows the peripheral arc transfer functions of the carotid sinus baroreflex estimated by the open-loop (left) and closed-loop (right) identification protocols in the ADN stimulation group. The top and middle panels are the gain and phase plots, respectively. In both transfer functions, the gain decreased as the frequency increased. The gain at the lowest frequency was slightly greater in the closed-loop than in the open-loop identification protocol. The phase at the lowest frequency indicated an in-phase relationship between SNA and AOP. The left-bottom panel shows the coherence function, which is a measure of the linear dependence between SNA and AOP in the frequency domain. The coherence was between 0.5 and 0.8. The identified transfer functions were virtually identical between the open-loop and closed-loop identification protocols. Furthermore, the estimated param-

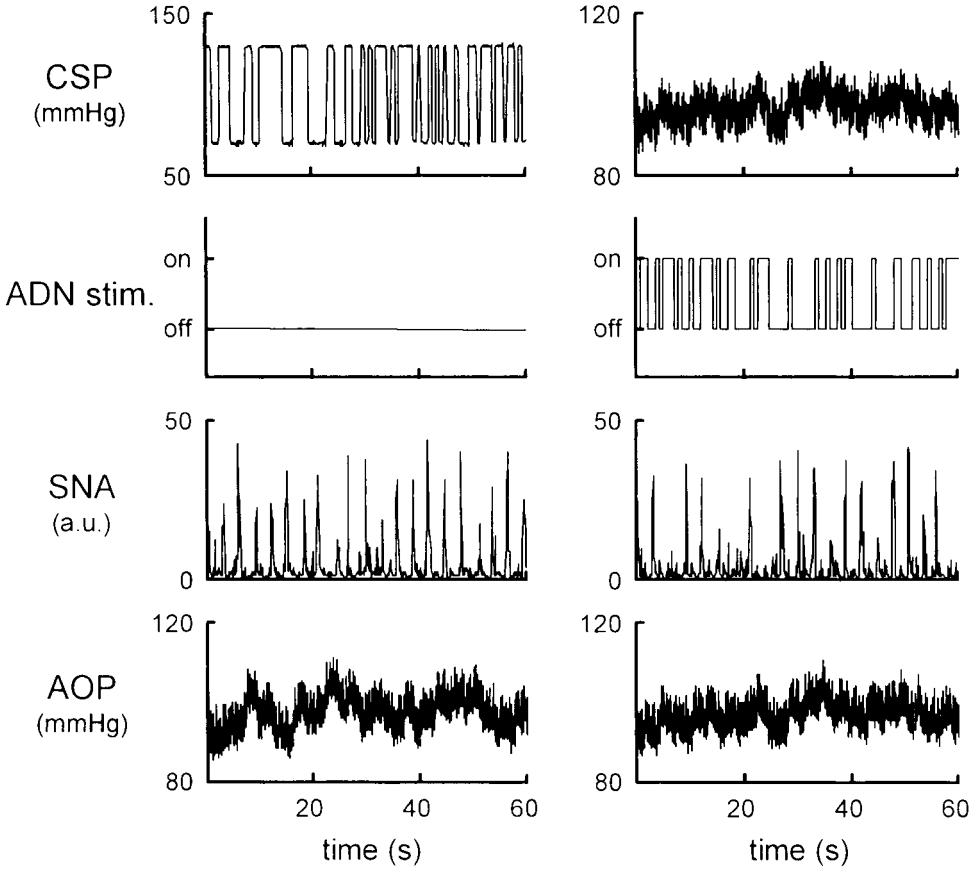

Fig. 2. Typical recordings of the open-loop (left) and closed-loop (right) identification protocols in the aortic depressor nerve (ADN) stimulation group. In the left panels, carotid sinus pressure (CSP) was perturbed according to a binary white noise sequence. Sympathetic nerve activity (SNA) and aortic pressure (AOP) changed in response to CSP perturbation. In the right panels, CSP was servo-controlled to precisely follow changes in AOP. ADN was stimulated according to a binary white noise sequence. SNA and AOP changed in response to ADN stimulation. Although SNA would also respond to changes in AOP, the absolute causality among signals could not be determined using the time series data.

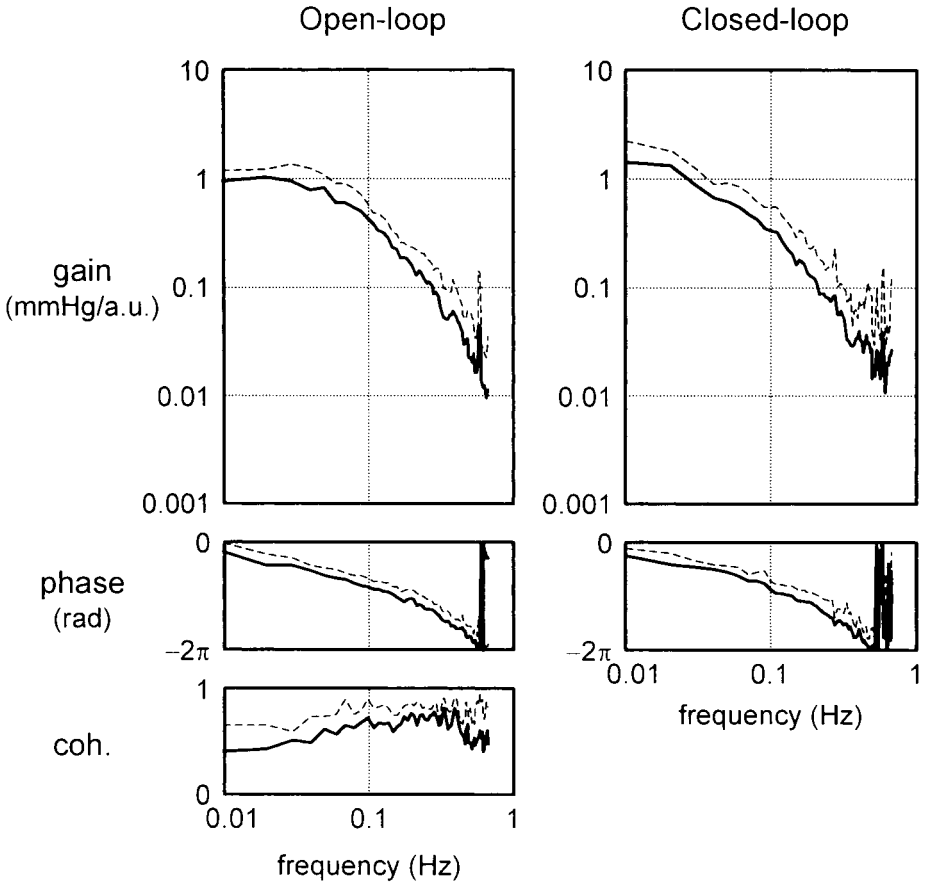

Fig. 3. Peripheral arc transfer functions of the carotid sinus baroreflex estimated by the open-loop (left) and closed-loop (right) identification protocols in the aortic depressor nerve stimulation group. Gain (**top**) and phase (**middle**) plots indicate low-pass filter characteristics of the peripheral arc transfer function. Solid and dashed lines indicate mean and mean+SD values, respectively. coh., magnitude squared coherence function.

Table 1. Fitted parameters of the peripheral arc transfer functions estimated by the open-loop and closed-loop identification protocols.

	Open-loop	Closed-loop	*p* value
Dynamic gain	1.02±0.11	1.16±0.32	0.71
Natural frequency (Hz)	0.092±0.033	0.084±0.029	0.88
Damping ratio	1.57±0.21	1.53±0.15	0.89
Lag time (s)	1.13±0.11	1.01±0.08	0.46

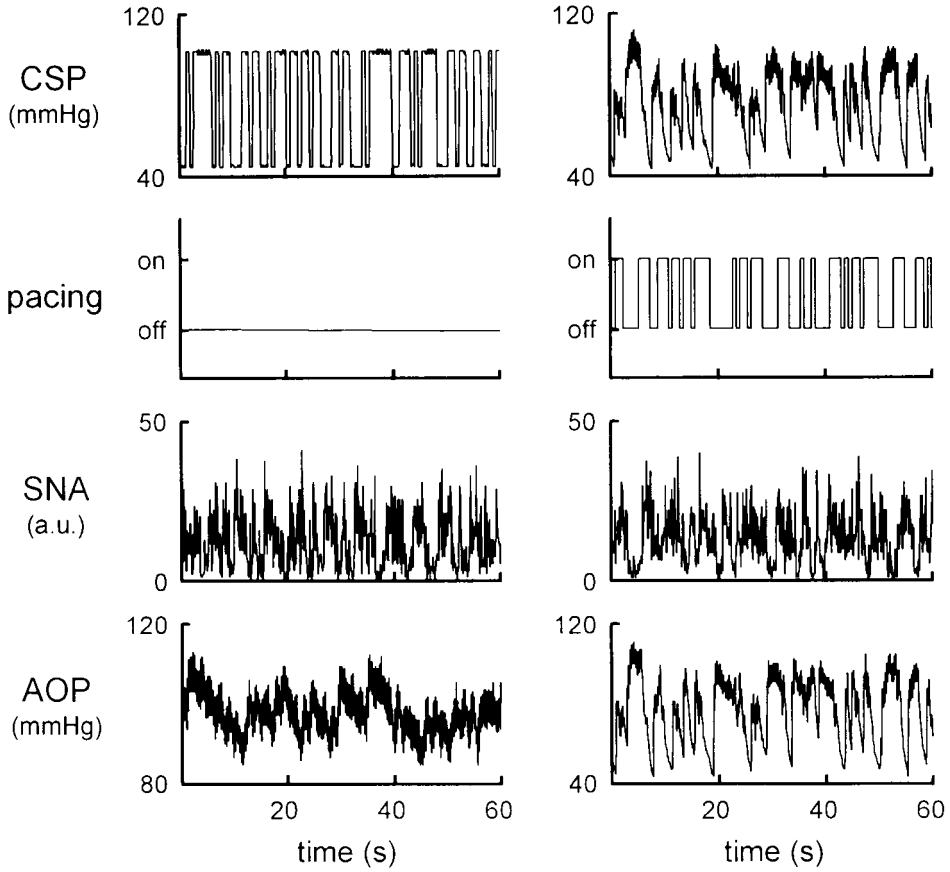

Fig. 4. Typical recordings of the open-loop (left) and closed-loop (right) identification protocols in the rapid pacing group. In the left panels, carotid sinus pressure (CSP) was perturbed according to a binary white noise sequence. Sympathetic nerve activity (SNA) and aortic pressure (AOP) changed in response to CSP perturbation. In the right panels, CSP was servo-controlled to precisely follow changes in AOP. Intermittent rapid pacing was applied according to a binary white noise sequence. AOP and SNA changed in response to rapid pacing. Although AOP would also respond to changes in SNA, the absolute causality among signals could not be determined using the time series data.

eters of the low-pass filter did not differ significantly between the open-loop and closed-loop identification protocols (Table 1).

Rapid pacing group

Figure 4 presents typical recordings obtained from the rapid pacing group, showing CSP, command signal for rapid pacing, SNA and AOP. The left and right panels correspond to the open-loop and closed-loop identification protocols, respectively. The open-loop identification protocol was similar to that shown in the ADN stimulation group (Fig. 2, left). However, the mean level of SNA was higher than that in the ADN stimulation group, reflecting low levels of CSP. In the closed-loop identification protocol, CSP was servo-controlled to precisely follow changes in AOP, thereby establishing baroreflex closed-loop conditions. We applied rapid pacing according to a binary white noise sequence. Rapid pacing decreased AOP, which reflexly increased SNA. Although changes in SNA would in turn alter AOP, the relationships among the command signal, SNA and AOP could not be differentiated based on the time series data.

Figure 5 shows the neural arc transfer functions of the carotid sinus baroreflex estimated by the open-loop (left) and closed-loop (right) identification protocols in the rapid pacing group. The top and middle panels are the gain and phase plots, respectively. In both transfer functions, the gain increased as the frequency increased. The increase in gain values was slightly more enhanced in the closed-loop than in the open-loop identification protocol. The phase showed a nearly out-of-phase relationship between CSP and SNA. The left-bottom panel is the coherence function,

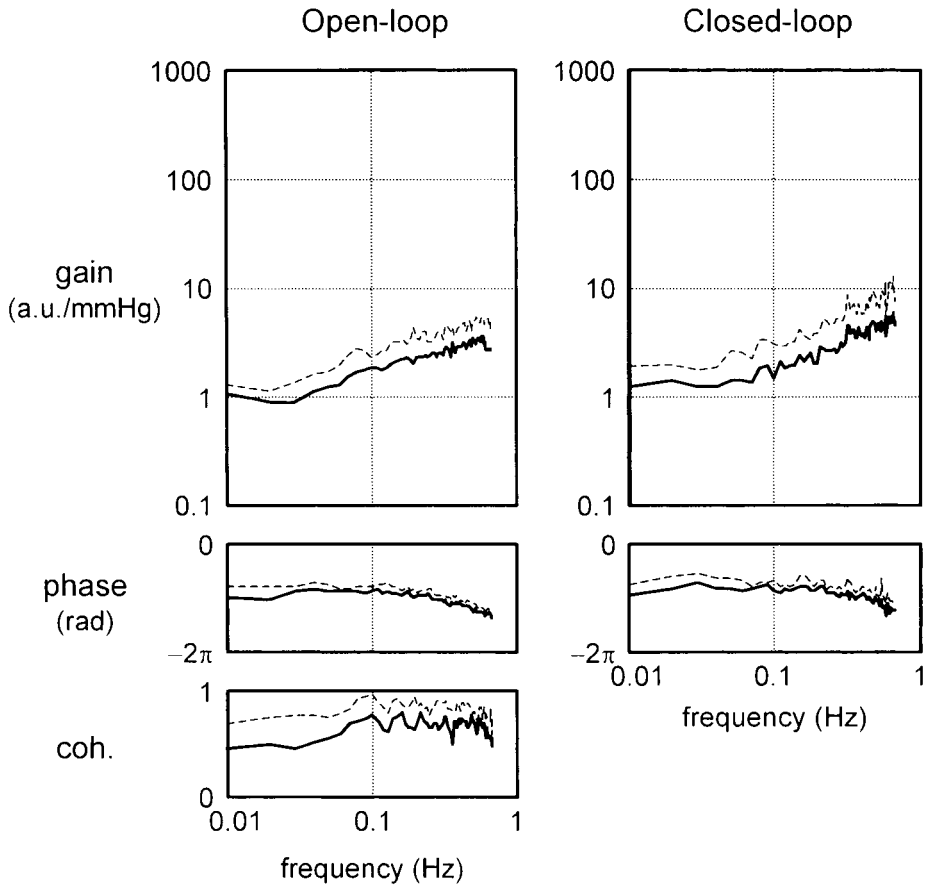

Fig. 5. Neural arc transfer functions of the carotid sinus-baroreflex estimated by the open-loop (left) and closed-loop (right) identification protocols in the rapid pacing group. Gain (**top**) and phase plots (**middle**) indicate high-pass filter characteristics of the neural arc transfer function. Solid and dashed lines indicate mean and mean+SD value, respectively. coh., magnitude squared coherence function.

Table 2. Fitted parameters of the neural arc transfer functions estimated by the open-loop and closed-loop identification protocols.

	Open-loop	Closed-loop	*p* value
Dynamic gain	−1.06±0.05	−1.15±0.45	0.87
Corner frequency (Hz)	0.13±0.03	0.12±0.05	0.83
Lag time (s)	0.50±0.08	0.44±0.25	0.84

showing the linear dependence between CSP and SNA. The coherence was between 0.5 and 0.8. The transfer functions estimated by the open-loop and closed-loop identification protocols were virtually indistinguishable. As a result, the estimated parameters of the high-pass filter did not differ significantly between the open-loop and closed-loop identification protocols (Table 2).

DISCUSSION

We have shown that ADN stimulation is an effective exogenous perturbation to estimate the peripheral arc transfer function under baroreflex closed-loop conditions. Similarly, rapid pacing is an effective exogenous perturbation to estimate the neural arc transfer function under baroreflex closed-loop conditions. Despite the fact that electrical stimulation was not a physiological input to the baroreflex system, we were able to obtain the baroreflex open-loop transfer functions in terms of two physiological parameters; namely blood pressure and SNA.

Closed-loop identification using ADN stimulation. The peripheral arc transfer function was estimated by the ADN stimulation protocol according to Eq. 6 under baroreflex closed-loop conditions. The estimated peripheral arc transfer function was comparable to that obtained by the open-loop identification protocol in its low-pass filter characteristics (Fig. 3, Table 1). Since the effective magnitude of exogenous perturbation differed between CSP perturbation and ADN stimulation, the system operating points of the open-loop and closed-loop identification protocols did not match exactly. The mean level of AOP was signifi-

cantly higher in the open-loop than in the closed-loop identification protocol (112.4±14.7 vs. 85.4±15.3 mmHg, $p<0.05$). The difference in the system operating points results in the difference in dynamic gain of the baroreflex [19]. However, as the input-output relationship between SNA and AOP is much more linear than that between CSP and SNA in the range from 80 to 120 mmHg [20], the differences in the system operating points might have minimally affected the dynamic gain of the peripheral arc transfer function.

As the closed-loop identification method was able to characterize the low-pass filter characteristics of the peripheral arc transfer function, we further examined whether the neural arc transfer function could be identified by ADN stimulation under baroreflex closed-loop conditions. First, we estimated $V(f)$ in Eq. 4 using AOP(f), SNA(f) and $H_P(f)$. Secondly, we calculated the ensemble average of crosspower between the terms of Eq. 3 and $V(f)$. Taking into account the statistical independence between $V(f)$ and $U(f)$ and that between $V(f)$ and $D(f)$, we obtained the following equation.

$$H_N(f)=\frac{E[S_{SNA\cdot V}(f)]}{E[S_{AOP\cdot V}(f)]}. \quad (9)$$

However, $H_N(f)$ estimated from Eq. 9 varied among animals and was inconsistent with the neural arc transfer function estimated by the open-loop identification protocol, such as that shown in Fig. 5. When applying Eq. 9, the identifiability of $H_N(f)$ depends critically on the property of $V(f)$. To obtain an unbiased estimate of $H_N(f)$, $V(f)$ should have sufficiently large power spectra over the entire frequency range of interest. Immobilization by anesthesia and muscular relaxant likely minimized the power of $V(f)$, thereby reducing the chance of correct $H_N(f)$ estimation.

The arterial baroreflex system reveals such non-linear system characteristics as threshold and saturation [20, 21]. Interactions between the carotid sinus and aortic baroreflexes have also been reported [22, 23]. However, the present results indicate that a linear system analysis worked reasonably well when used to examine the system characteristics around the physiological operating pressure. As the afferent signals elicited by ADN stimulation and CSP perturbation converge initially on the dorsomedial portions of the nucleus of the tractus solitarius [24], $H_D(f)$ and $H_N(f)$ in Fig. 1A are not anatomically independent elements. If the afferent signals elicited by ADN stimulation and CSP perturbation interfere strongly with one another in the central pathways of the baroreflex, linearity between the command sequence of ADN stimulation and SNA would decrease, resulting in decreased accuracy of the $H_P(f)$ estimation by Eq. 6. Judging from the accurate $H_P(f)$ estimation under baroreflex closed-loop conditions (Fig. 3, Table 1), we postulate that the dynamic interaction in the central pathways between the carotid sinus and aortic baroreflexes was sufficiently small to allow the system to obey linear system dynamics in the present study.

Closed-loop identification using rapid pacing. The neural arc transfer function was estimated by rapid pacing according to Eq. 8 under baroreflex closed-loop conditions. The estimated neural arc transfer function was comparable to that estimated by the open-loop identification protocol (Fig. 5, Table 2). The high-pass characteristics, however, appear to be more enhanced in the closed-loop than in the open-loop identification protocol. The spectrum of AOP gradually lost its power beyond 0.2 Hz due to a delay in the AOP response to rapid pacing in the closed-loop identification protocol. In contrast, the spectrum of CSP was fairly flat up to 0.7 Hz in the open-loop identification protocol. The transfer gain becomes small as the input amplitude increases due to a nonlinear sigmoidal input-output relationship in the arterial baroreflex system [2]. The slight enhancement of high-pass characteristics in the closed-loop identification protocol might therefore be attributable to a difference in the power spectrum of effective baroreceptor input between the open-loop and closed-loop identification protocols.

We will discuss the inability of a conventional open-loop identification method to estimate the neural arc transfer function under baroreflex closed-loop conditions. Calculating the ensemble average of crosspower between the terms of Eq. 7 and AOP(f), we obtain:

$$E[S_{SNA\cdot AOP}(f)]=H_N(f)E[S_{AOP\cdot AOP}(f)]+E[S_{U\cdot AOP}(f)]. \quad (10)$$

Rearranging Eq. 10 for $H_N(f)$, we obtain:

$$H_N(f)=\frac{E[S_{SNA\cdot AOP}(f)]}{E[S_{AOP\cdot AOP}(f)]}-\frac{E[S_{U\cdot AOP}(f)]}{E[S_{AOP\cdot AOP}(f)]}. \quad (11)$$

The first term of Eq. 11 conforms to Eq. 1 when we treat AOP(f) as the input and SNA(f) as the output of the system. However, $E[S_{U\cdot AOP}(f)]$ in the second term of Eq. 11 does not disappear as long as $U(f)$ affects AOP(f) through the peripheral arc. Therefore, the conventional open-loop identification method yields an erroneous estimation of $H_N(f)$ when applied under baroreflex closed-loop conditions.

We have demonstrated that exogenous arterial pressure perturbation can be used to estimate the periph-

eral arc as well as the neural arc transfer functions in a previous study [5]. Rapid pacing is similar to arterial blood withdrawal and infusion in the sense that it primarily perturbs AOP. However, in contrast to arterial blood withdrawal and infusion, rapid pacing cannot be used to estimate the peripheral arc transfer function under baroreflex closed-loop conditions. As mentioned in the MATERIALS AND METHODS section, because rapid pacing deprives the peripheral arc of the heart rate control component, $H_P(f)$ in Fig. 1B becomes time variant. Therefore, analysis for a linear time invariant system is not applicable to the $H_P(f)$ estimation during intermittent rapid pacing.

Limitations. There are several limitations to the present study. First, we performed the experiment in animals under anesthetic conditions, since the open-loop identification protocol was required to verify the results of the closed-loop identification protocol. The system gain might have been differently estimated if we had performed the experiment using animals under conscious conditions.

Second, to simplify the framework of the closed-loop system identification, we sectioned vagi and eliminated the low-pressure baroreflex from the cardiopulmonary regions. When applying the closed-loop identification method using electrical stimulation in conscious animals, temporary interruption of the vagi would be necessary. Local anesthesia and nerve cooling have previously been used for this purpose [25, 26].

Third, we represented SNA responsible for the arterial pressure regulation by the left cardiac SNA. As regional differences in SNA might exist in response to changes in CSP, utilizing SNA related to other neural districts such as the renal SNA and splanchnic SNA might affect the estimation of the neural and peripheral arc transfer functions. However, the tight linear relationship between CSP and cardiac SNA and between cardiac SNA and AOP, as evidenced by the relatively high coherence values in the open-loop identification protocols (Fig. 3, left, and Fig. 5, left), enabled us to use cardiac SNA to precisely estimate the neural and peripheral arc transfer functions.

Finally, we filled the isolated carotid sinuses with warmed physiological saline. As the ion content affects the sensitivity of baroreceptors [27], the absolute gain values of the carotid sinus baroreflex might have been different had we used a different solution, such as Ringer's solution. The extent of chemoreceptor activation might also affect SNA and AOP or interfere with the carotid sinus baroreflex. However, we changed neither the intravascular ion content nor O_2 content of the isolated carotid sinuses between the open-loop and closed-loop identification protocols. Thus, a comparison of the transfer functions between the open-loop and closed-loop identification protocols might be fair.

Conclusion. The present study established the efficacy of the non-parametric frequency-domain closed-loop identification method using electrical stimulation in estimating baroreflex open-loop transfer functions. We isolated the carotid sinuses in order to compare the results of the closed-loop identification method with those of the open-loop identification method. However, the isolation of the carotid sinuses is not essential when we apply the closed-loop identification method alone. We can therefore estimate dynamic characteristics of the arterial baroreflex while preserving physiological conditions around the baroreceptor regions. Although we separately applied ADN stimulation and rapid pacing in different groups of animals, these exogenous perturbations can be combined in the same animal. Given that wireless electrical stimulation is available by implanting an electrical stimulator with a small battery, the developed framework should provide a useful strategy in estimating baroreflex open-loop transfer functions in freely moving animals.

This study was supported by Research Grants for Cardiovascular Diseases (9C-1, 11C-3, 11C-7) from the Ministry of Health and Welfare of Japan, by a Health Sciences Research Grant for Advanced Medical Technology from the Ministry of Health and Welfare of Japan, by Special Funds for Encouragement System of COE from the Science and Technology Agency of Japan, by a Ground-Based Research Grant for the Space Utilization promoted by NASDA and the Japan Space Forum, by a Bilateral International Joint Research Grant from the Science and Technology Agency of Japan, by Grant-in-Aid for Scientific Research (B: 11694337, C: 11680862, 11670730) and Grant-in-Aid for Encouragement of Young Scientists (11770390, 11770391) from the Ministry of Education, Science, Sports and Culture of Japan, and by a grant provided by the Ichiro Kanehara Foundation.

REFERENCES

1. Ikeda Y, Kawada T, Sugimachi M, Kawaguchi O, Shishido T, Sato T, Miyano H, Matsuura W, Alexander J Jr, and Sunagawa K: Neural arc of baroreflex optimizes dynamic pressure regulation in achieving both stability and quickness. Am J Physiol 271: H882–H890, 1996
2. Kawada T, Fujiki N, and Hosomi H: Systems analysis of the carotid sinus baroreflex system using a sum-of-sinusoidal input. Jpn J Physiol 42: 15–34, 1992
3. Suga H and Oshima M: Measurement of the transfer function of the carotid sinus pressure control system with its feedback loop physiologically closed. Med Biol Eng 9: 147–150, 1971
4. Hosomi H and Yokoyama K: Estimation of open-loop

gain of canine arterial pressure control system by a new method. Am J Physiol 240: H832–H836, 1981
5. Kawada T, Sugimachi M, Sato T, Miyano H, Shishido T, Miyashita H, Yoshimura R, Takaki H, Alexander J Jr, and Sunagawa K: Closed-loop identification of carotid sinus baroreflex open-loop transfer characteristics in rabbits. Am J Physiol 273: H1024–H1031, 1997
6. Kubo T, Imaizumi T, Harasawa Y, Ando S, Tagawa T, Endo T, Shiramoto M, and Takeshita A: Transfer function analysis of central arc of aortic baroreceptor reflex in rabbits. Am J Physiol 270: H1054–H1062, 1996
7. Sugimachi M, Imaizumi T, Sunagawa K, Hirooka Y, Todaka K, Takeshita A, and Nakamura M: A new method to identify dynamic transduction properties of aortic baroreceptors. Am J Physiol 258: H887–H895, 1990
8. Marmarelis PZ and Marmarelis VZ: The white noise method in system identification. *In*: Analysis of Physiological Systems, Plenum Press, New York, pp 131–221, 1978
9. Kawada T, Sato T, Shishido T, Inagaki M, Tatewaki T, Yanagiya Y, Sugimachi M, and Sunagawa K: Summation of dynamic transfer characteristics of left and right carotid sinus baroreflexes in rabbits. Am J Physiol 277: H857–H865, 1999
10. Miyano H, Nakayama Y, Shishido T, Inagaki M, Kawada T, Sato T, Miyashita H, Sugimachi M, Alexander J Jr, and Sunagawa K: Dynamic sympathetic regulation of left ventricular contractility studied in the isolated canine heart. Am J Physiol 275: H400–H408, 1998
11. Sato T, Kawada T, Shishido T, Miyano H, Inagaki M, Miyashita H, Sugimachi M, Knuepfer MM, and Sunagawa K: Dynamic transduction properties of *in situ* baroreceptors of rabbits aortic depressor nerve. Am J Physiol 274: H358–H365, 1998
12. Sato T, Kawada T, Shishido T, Sugimachi M, Alexander J Jr, and Sunagawa K: Novel therapeutic strategy against central baroreflex failure. A bionic baroreflex system. Circulation 100: 299–304, 1999
13. Harris FJ: On the use of windows for harmonic analysis with the discrete Fourier transform. Proc IEEE 66: 51–83, 1978
14. Brigham EO: FFT transform applications. *In*: The Fast Fourier Transform and Its Applications, Prentice-Hall, Englewood Cliffs, NJ, pp 167–203, 1988
15. Söderström T and Stoica P: Identification of systems operating in closed loop. *In*: System Identification, Prentice Hall, Englewood Cliffs, NJ, pp 381–421, 1989
16. Miyano H, Kawada T, Shishido T, Sato T, Sugimachi M, Alexander J Jr, and Sunagawa K: Inhibition of NO synthesis minimally affects the dynamic baroreflex regulation of sympathetic nerve activity. Am J Physiol 272: H2446–H2452, 1997
17. Miyano H, Kawada T, Sugimachi M, Shishido T, Sato T, Alexander J Jr, and Sunagawa K: Inhibition of NO synthesis does not potentiate dynamic cardiovascular response to sympathetic nerve activity. Am J Physiol 273: H38–H43, 1997
18. Glantz SA: Primer of Biostatistics, 4th ed, McGraw-Hill, New York, pp 65–107, 1997
19. Parati G, Saul JP, Rienzo MD, and Mancia G: Spectral analysis of blood pressure and heart rate variability in evaluating cardiovascular regulation. A critical appraisal. Hypertension 25: 1276–1286, 1995
20. Sato T, Kawada T, Inagaki M, Shishido T, Takaki H, Sugimachi M, and Sunagawa K: New analytical framework for understanding sympathetic baroreflex control of arterial pressure. Am J Physiol 277: H2251–H2261, 1999
21. Kent BB, Drane JW, Blumenstein B, and Manning JW: A mathematical model to assess changes in the baroreceptor reflex. Cardiology 57: 295–310, 1972
22. Hosomi H, Katsuda S, Morita H, Nishida Y, and Koyama S: Interactions among reflex compensatory systems for posthemorrhage hypotension. Am J Physiol 250: H944–H953, 1986
23. Ishikawa N and Sagawa K: Nonlinear summation of depressor effects of carotid sinus pressure changes and aortic nerve stimulation in the rabbit. Circ Res 52: 401–410, 1983
24. Andresen MC and Kunze DL: Nucleus tractus solitarius. Gateway to neural circulatory control. Annu Rev Physiol 56: 93–116, 1994
25. Stone HL and Bishop VS: Ventricular output in conscious dogs following acute vagal blockade. J Appl Physiol 24: 782–786, 1968
26. Clement DL, Pelletier CL, and Shepherd JT: Role of vagal afferents in the control of renal sympathetic nerve activity in the rabbit. Circ Res 31: 824–830, 1972
27. Andresen MC and Kunze DL: Ionic sensitivity of baroreceptors. Circ Res 61 (Suppl): I66–I71, 1987

APPENDIX

High-pass and low-pass filters used for the parameterization of the transfer functions

We fitted a first-order high-pass filter to the neural arc transfer function of the carotid sinus baroreflex. The first-order high-pass filter is expressed in the frequency domain as

$$H_{\mathrm{N}}(f)=-K\left(1+\frac{f}{f_0}\right)\mathrm{e}^{-2\pi fjL},$$

where K, f_0 and L are dynamic gain, corner frequency (in Hz) and lag time (in s), respectively. f denotes frequency (in Hz). j is the imaginary unit. The negative sign of K indicates negative feedback through the neural arc.

We fitted a second-order low-pass filter to the peripheral arc transfer function of the carotid sinus baroreflex. The second-order low-pass filter is expressed in the frequency domain as:

$$H_{\mathrm{P}}(f)=\frac{K}{1+2\zeta\frac{f}{f_0}j-\left(\frac{f}{f_0}\right)^2}\mathrm{e}^{-2\pi fjL}$$

where K, f_0, ζ and L are dynamic gain, natural frequency (in Hz), damping ratio and lag time (in s), respectively. f denotes frequency (in Hz). j is the imaginary unit.